

Singly resonant optical parametric oscillation in periodically poled lithium niobate waveguides

M. A. Arbore and M. M. Fejer

E. L. Ginzton Laboratory, Stanford University, Stanford, California 94305

Received September 13, 1996

We report quasi-phase-matched singly resonant optical parametric oscillation in electric-field-poled lithium niobate waveguides. Parametric gains as high as 250%/W, an oscillation threshold of 1.6 W (peak), idler output powers of 220 mW, and a tuning range of 1180–2080 nm for pump wavelengths of 756–772 nm have been observed. Pump depletion is limited to 40% because of the multiple launched transverse modes at the pump wavelength. We predict that fully optimized waveguide singly resonant oscillators can have thresholds of ~100 mW, accessible to cw diode pumping. © 1997 Optical Society of America

Efficient low-power compact sources of tunable coherent near- and mid-infrared wavelength radiation are necessary for many applications, including communications, spectroscopy, and process monitoring. Optical parametric oscillators (OPO's) offer extremely wide tunability intrinsically limited only by material transparency, require only a single pump laser, and offer an energy conversion efficiency much larger than that of single-pass nonlinear interactions such as difference-frequency generation.¹ Although doubly resonant oscillators, with feedback at both the signal and the idler wavelength, can have low thresholds, their tuning behavior is complicated. Singly resonant oscillators (SRO's), with feedback only at the signal wavelength, offer simplified tuning at the expense of higher thresholds. One current challenge for practical OPO's is reducing the oscillation threshold to levels attainable with diode lasers.

Waveguide geometries increase conversion efficiencies of nonlinear devices by tightly confining the optical fields over long interaction lengths. Several guided-wave nonresonant interactions including parametric fluorescence² and highly efficient second-harmonic generation³ (SHG) and difference-frequency generation⁴ have been reported; however, practical waveguide OPO's require several materials issues to be solved, particularly the simultaneous realization of tightly confining low-loss and axially homogeneous waveguide structures. All experimental realizations of guided-wave OPO's to date have been used in LiNbO₃ crystals because of the availability of waveguide technologies that can meet some of these requirements while using large nonlinear coefficients. Birefringently phase matched 7.6-W threshold singly resonant⁵ and 27-mW threshold doubly resonant⁶ OPO's have been demonstrated in low-loss Ti-diffused LiNbO₃ waveguides. These devices operated at temperatures between 170 and 230 °C with pump wavelengths of ≈600 nm and parametric gains⁷ of 9%/W (normalized parametric gain $\eta_{\text{nor}} = 0.5\%/W \text{ cm}^2$). The previously reported quasi-phase-matched waveguide OPO⁸ was pumped at room temperature at ≈780 nm, had a parametric gain of $\eta = 18\%/W$ ($\eta_{\text{nor}} = 22\%/W \text{ cm}^2$), and had an oscillation threshold of 4 W. Since then, processing

improvements have resulted in an order-of-magnitude improvement in parametric gain, a 2.5-fold reduction in oscillation threshold, and true singly resonant operation. We report these device improvements, detailed characterization of OPO performance, and a proposal to integrate adiabatic waveguide tapers into the SRO to reduce the oscillation threshold further and to increase device robustness.

The pump threshold for parametric oscillation in a symmetric resonator with equal signal and idler losses is⁹

$$P_{\text{th}} = \frac{1}{r\eta_{\text{nor}}} \left[\frac{\alpha_p}{1 - \exp(-\alpha_p L)} \ln \left(Q + \sqrt{Q^2 - 1} \right) \right]^2, \quad (1)$$

with

$$Q = \frac{1 + R_s R_i \exp(-4\alpha L)}{(R_s + R_i) \exp(-2\alpha L)}, \quad (2)$$

where r is the fraction of pump power launched in the phase-matched transverse mode, α_p is the field loss coefficient at the pump wavelength, $R_{s,i}$ and α are the mirror power reflectivities and the field loss coefficient at the signal and the idler wavelengths, respectively, and η_{nor} is the normalized small-signal parametric gain (expressed in units of %/W cm²). For low-finesse resonators, such as those containing moderate-loss tightly confining waveguides, the threshold of a SRO does not significantly exceed that of a doubly resonant oscillator.

A significant difference between bulk and waveguide OPO's is that waveguide modes are generated and depleted as entities, so they evolve in the same way as in plane-wave devices. In particular, the pump transmission T can be written as¹⁰

$$T = r \cos^2(\Gamma) + (1 - r), \quad \sin^2(\Gamma)/\Gamma^2 = P_t/P, \quad (3)$$

where P and P_t are pump power and threshold pump power, respectively. Waveguide SRO's exhibit 100% depletion of the pump mode for pumping at $(\pi/2)^2$ times above threshold power.

The channel waveguide device reported here was designed with the models for linear and nonlinear properties of annealed proton-exchange (APE) LiNbO₃ given in Ref. 11 to have a normalized parametric gain of 85%/W cm² and only two transverse modes at degeneracy. A normalized gain of 100%/W cm² is predicted for a more tightly confining (but also highly multimoded) waveguide optimized for gain.

A 7.6-cm-diameter, 0.5-mm-thick *z*-cut wafer of congruent LiNbO₃ was lithographically patterned on the +*z* (+*c*) face with a 2.5- μ m-thick, 14- μ m-period grating of photoresist (Shipley 1400-33) with 4- μ m-wide openings. A 50-nm-thick film of chrome was sputtered over the center 6 cm. The wafer was then poled¹² with an electric field of \sim 20.5 kV/mm at a regulated current of 23 mA for 100 ms. The resulting full-wafer domain pattern had \sim 10% of domains missing and local duty cycles of \sim 35–65%. The sample was proton exchanged in pure benzoic acid at 177 °C for 3.9 h, to a depth of 0.55 μ m, through a lithographically defined mask of sputtered SiO₂ with 5- μ m-wide channel openings. The 2.7-cm-long sample was annealed in air at 340 °C for 11.5 h, resulting in phase matching of SHG or a degenerate OPO at 1543 nm.

A single-frequency SHG tuning curve (Fig. 1) for the best waveguide on the sample exhibited a near-sinc² shape, a 0.5-nm FWHM bandwidth (indicating phase matching over 2.4 cm), and a peak internal conversion efficiency η of 250%/W, corresponding to 43%/W cm². We investigated the efficiency and phase-matching behavior of single-pass parametric gain, using a self-injection-seeded acousto-optically *Q*-switched (at 100 Hz to minimize photorefractive effects) Ti:sapphire laser with \sim 100 ns FWHM, $<$ 0.1-nm-bandwidth output pulses as a pump source, and a 1.32 μ m cw Nd:YAG laser as a signal source. With high launched peak pump powers of \sim 4 W, a maximum single-pass gain of 20 dB was observed, limited by the onset of oscillation caused by feedback from the Fresnel reflections off the uncoated waveguide end faces.

A waveguide supporting a mode at the idler wavelength is of necessity highly multimoded at the pump wavelength; in this case, more than 13 modes were supported at 770 nm. Even with careful input coupling it is difficult to avoid significant launching of pump power into high-order modes. The observed small-signal parametric gains are consistent with the measured SHG efficiency and $r \approx 0.5$.

A similar waveguide from the same sample with a gain of 175%/W was used for the OPO experiments. Waveguide losses at 1.32 μ m of 0.6 dB/cm ($\alpha = 0.069$ cm⁻¹) were measured by the Fabry–Perot method.¹³ Dielectric mirrors with high reflectivity from 1100 to 1475 nm and $<$ 5% reflectivity for $\lambda >$ 1600 nm (to ensure SRO operation) were placed in contact with the waveguide end faces; this simple mounting scheme caused \sim 2% loss per mirror. Equation (1) indicates a 620-mW threshold for this device near degeneracy, assuming $r = 1$ and equal waveguide losses at all wavelengths. Idler and pump losses below \sim 1 dB/cm do not significantly affect the singly resonant threshold.

Using the same pump source as above, we observed an oscillation threshold of 1.6 (peak) W of launched power, consistent with the predicted threshold if $r = 0.38$; all SRO measurements were made with similar pump launching conditions. The spectral linewidth, averaged over many pulses, of the idler was \sim 4 nm. Tuning the pump wavelength from 756 to 772 nm tuned the SRO output wavelengths over 1180–2080 nm, as shown in Fig. 2. The solid curve is a prediction based on the theoretical waveguide dispersion, with the degeneracy wavelength set to the measured value. This measurement extends the linear APE model for Ref. 11 through the near IR.

Figure 3 shows pump transmission and peak idler output power as a function of peak launched pump power. The curve is a fit to Eq. (3), giving $r = 0.42$. The maximum pump depletion, observed at 1700 nm, was 40%, with a peak launched pump power of 3.7 W (2.1 times threshold) and a peak idler output power of 220 mW. Note that the observed 40% pump depletion implies \sim 95% depletion of the pump power in the phase-matched mode, assuming that $r = 0.42$.

Figure 4 shows the measured relative oscillation threshold plotted against the ratio of idler-to-signal

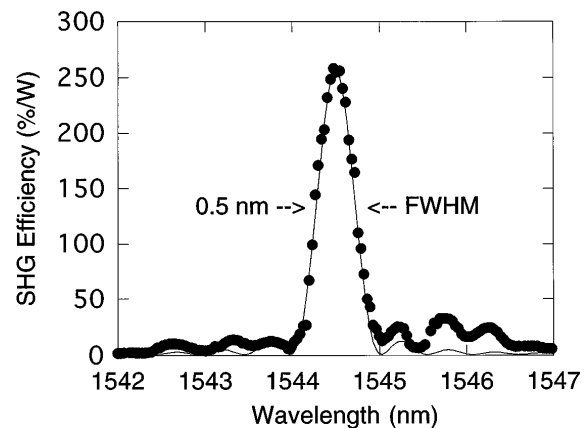


Fig. 1. Single-frequency SHG tuning curve. The peak efficiency is identical to the near-degenerate parametric gain. The solid curve is a fit to $\sin^2(x)/x^2$.

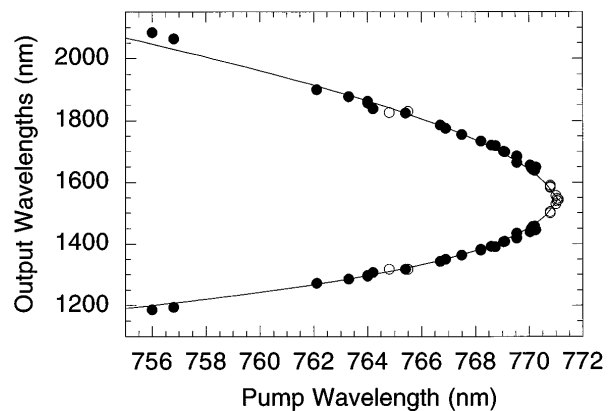


Fig. 2. Parametric tuning curve for a waveguide SRO (filled circles). Data near degeneracy (open circles) was measured by SHG and single-pass parametric gain. The solid curve is a theoretical prediction.

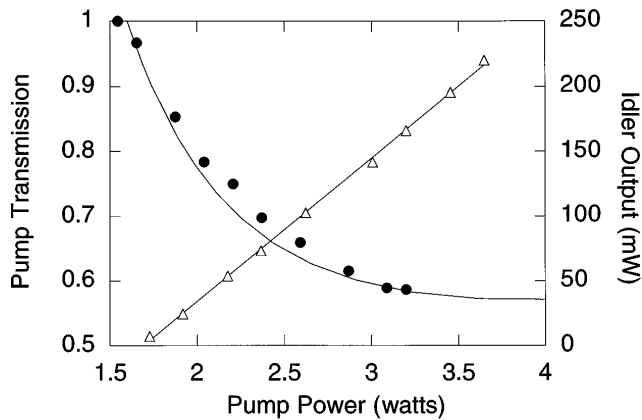


Fig. 3. SRO pump depletion (circles) and output power (triangles) versus peak launched pump power. The curve is a fit to Eq. (3), giving $r = 0.42$.

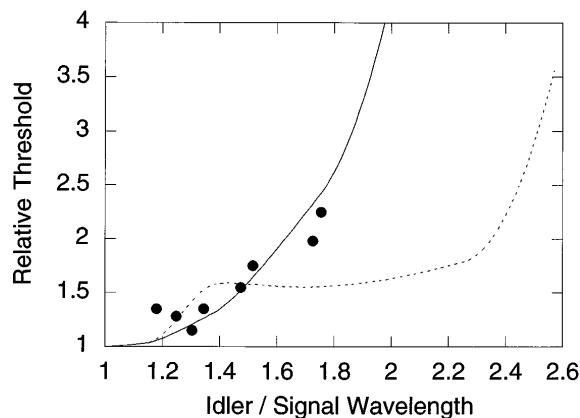


Fig. 4. Relative SRO threshold versus operating wavelength. The filled circles are measured values; the solid and dashed curves are theoretical predictions for the fabricated device and for an alternative design optimized for off-degenerate operation, respectively.

wavelength λ_i/λ_s . The solid curve is a theoretical prediction of pump threshold for the device fabricated, based on Eq. (1), $r = 0.40$, a wavelength-dependent value of η_{nor} derived from Ref. 11, the measured 175-%/W degenerate gain, and 0.6-dB/cm losses at all wavelengths. The agreement between experimental and theoretical thresholds indicates that the same APE LiNbO₃ model can be used to predict the threshold of alternative design (dashed curve in Fig. 4) optimized for off-degenerate operation.

It has been shown that a segmented waveguide (used for pump launching) that is single moded at both the pump and the signal wavelengths can be integrated with an adiabatic taper¹⁴ and a waveguide that tightly confines the idler wavelength, provided that the parametric device is operated off degeneracy,⁴ eliminating the pump mode launching problem and guaranteeing that $r \approx 1$. The oscillation threshold for such a waveguide SRO can be predicted by Eq. (1) if the single-pass transmission of the taper to the signal wavelength is included in the effective mirror reflectivity R_s . From Ref. 15 one finds that 14% excess

loss is typical, though not necessarily minimum; using this figure, the wavelength scaling of parametric gain discussed above, our highest observed normalized degenerate gain of 43%/W cm², and our lowest observed loss of 0.4 dB/cm, we predict a singly resonant oscillation threshold for a 3-cm device of 480 mW. APE LiNbO₃ waveguides with losses of 0.2 dB/cm have been reported,¹⁵ though it has not been shown that these losses are compatible with the tight confinement required for high gain. Assuming these losses and an optimized normalized gain of 100%/W cm², we predict a singly resonant oscillation threshold for a 3-cm device of 130 mW, clearly accessible to diode-laser pumping. Future studies will investigate such optimized devices.

The authors acknowledge generous donation of materials from Crystal Technology and mirrors from Spectra-Physics. We appreciate helpful discussions with G. D. Miller, L. E. Myers, M. H. Chou, and M. L. Bortz. This research was supported by the Defense Advanced Research Projects Agency through the Center for Nonlinear Optical Materials and by the Joint Services Electronics Program.

References

1. See the feature on parametric devices, *J. Opt. Soc. Am. B* **12**, 2084–2320 (1995).
2. P. Baldi, P. Aschieri, S. Nouh, M. De Micheli, D. Ostrowsky, D. Delacourt, and M. Papuchon, *IEEE J. Quantum Electron.* **31**, 997 (1995).
3. K. Kintaka, M. Fujimura, T. Suhara, and H. Nishihara, *J. Lightwave Technol.* **14**, 462 (1996).
4. M. A. Arbore, M. H. Chou, and M. M. Fejer, in *Conference on Lasers and Electro-Optics*, Vol. 9 of 1996 OSA Technical Digest Series (Optical Society of America, Washington, D.C., 1996), p. 120.
5. W. Sohler and H. Suche, in *Digest of the Third International Conference on Integrated Optics and Optical Fiber Communication* (Optical Society of America, Washington, D.C., 1981), p. 89.
6. H. Suche and W. Sohler, in *Integrated and Guided-Wave Optics*, Vol. 5 of 1988 OSA Technical Digest Series (Optical Society of America, Washington, D.C., 1988), p. 176.
7. W. Sohler and H. Suche, *Appl. Phys. Lett.* **37**, 255 (1980).
8. M. L. Bortz, M. A. Arbore, and M. M. Fejer, *Opt. Lett.* **20**, 49 (1995).
9. G. P. Bava, I. Montrosset, W. Sohler, and H. Suche, *IEEE J. Quantum Electron.* **QE-23**, 42 (1987).
10. J. E. Bjorkholm, *IEEE J. Quantum Electron.* **QE-7**, 109 (1971).
11. M. L. Bortz and M. M. Fejer, *Opt. Lett.* **16**, 1844 (1991); M. L. Bortz, L. A. Eyres, and M. M. Fejer, *Appl. Phys. Lett.* **62**, 2012 (1993).
12. L. E. Myers, R. C. Eckardt, M. M. Fejer, R. L. Byer, W. R. Bosenberg, and J. W. Pierce, *J. Opt. Soc. Am. B* **12**, 2102 (1995); G. D. Miller, R. G. Batchko, M. M. Fejer, and R. L. Byer, *Proc. SPIE* **2700**, 34 (1996).
13. R. Regener and W. Sohler, *Appl. Phys. B* **36**, 143 (1985).
14. M. H. Chou, M. A. Arbore, and M. M. Fejer, *Opt. Lett.* **21**, 794 (1996).
15. G. A. Bogert and D. T. Moser, *IEEE Photon. Technol. Lett.* **12**, 632 (1990).